RI 7653

Bureau of Mines Report of Investigations/ 1972

# Ground Vibrations From Tunnel Blasting in Granite

## Cheyenne Mountain (NORAD), Colo.

UNITED STATES DEPARTMENT OF THE INTERIOR

Report of Investigations 7653

# Ground Vibrations From Tunnel Blasting in Granite

## Cheyenne Mountain (NORAD), Colo.

By James J. Olson, David E. Fogelson, Richard A. Dick, and Arlo D. Hendrickson
Twin Cities Mining Research Center, Minneapolis, Minn.

UNITED STATES DEPARTMENT OF THE INTERIOR
Rogers C. B. Morton, Secretary

BUREAU OF MINES
Elburt F. Osborn, Director

This publication has been cataloged as follows:

Olson, James J

Ground vibrations from tunnel blasting in granite: Cheyenne Mountain (NORAD), Colo., by James J. Olson [and others. Washington] U.S. Dept. of the Interior, Bureau of Mines [1972]

25 p. illus., tables. (U.S. Bureau of Mines. Report of investigations 7653)

Includes bibliography.

1. Granite industry and trade—Cheyenne Mountain, Colo.—NORAD Complex. 2. Tunneling—Blast effect. I. Title. (Series)

TN23.U7 no. 7653 622.06173

U.S. Dept. of the Int. Library

CONTENTS



ILLUSTRATIONS



TABLES

# GROUND VIBRATIONS FROM TUNNEL BLASTING IN GRANITE

## Cheyenne Mountain (NORAD), Colo.

by

James J. Olson,[1] David E. Fogelson,[2] Richard A. Dick,[1]
and Arlo D. Hendrickson[3]

## ABSTRACT

The Bureau of Mines recorded peak particle-velocity levels and vibration frequencies to determine the nature and intensity of ground vibrations for tunnel blast rounds at the NORAD Complex, Colorado Springs, Colo. Previous Bureau of Mines studies in quarries and underground mines had shown that scaling (dividing) the distance from the blast by the square root of the charge weight removed the effect of the various charge weights on vibration amplitudes. The analysis of variance tests performed on the NORAD vibration data, however, indicated that the cube rather than square root scaling exponent grouped the data more effectively. The empirical propagation equation, $V = 560\ (D/W^{1/3})^{-2.04}$, where V is the maximum peak particle velocity in inches per second, D is the distance from the blast in feet, and W is the zero-delay charge weight in pounds described the attenuation, with distance, of the particle velocities from the tunnel blasts in the Pikes Peak Granite of the NORAD Complex.

## INTRODUCTION

At the request of the U.S. Army Corps of Engineers, the Bureau recorded ground vibrations from blasts used to excavate an exploratory drift at the North American Air Defense Command (NORAD) Complex, Cheyenne Mountain, Colo. The purpose of the investigation was to determine the amplitudes and frequencies of ground motion and to develop an empirical prediction equation for vibration amplitudes produced by various sizes of tunnel blasts in granite. During the subsequent expansion of the exploratory drift into a chamber, the Corps of Engineers used the prediction equation to design blast rounds that would not generate excessive vibration levels. The NORAD study also constituted a continuation of the Bureau's investigations of blast vibrations under different underground conditions.

---

[1]Mining engineer.

[2]Supervisory geophysicist.

[3]Mathematician (now Assistant Professor of Applied Statistics, Virginia Polytechnic Institute and State University, Blacksburg, Va.).

Tunnels for construction or mining projects have historically been excavated by two principal methods: machine boring or explosive fragmentation (drill-blast). During recent years, increased efforts have been made to use excavation methods not affected by the noncontinuous aspects inherent in the drill-blast cycle. Hydraulic mining methods have achieved acceptable penetration rates in excavating soft rock formations. In addition, coal mine production openings are often made with highly efficient continuous-mining machines. For long tunnels in relatively soft, nonabrasive rocks, cutter costs and downtime are usually not excessive, and the boring machine has virtually replaced the drill-blast method.

When variable conditions such as a mixed face, squeezing ground, or excessive ground water are encountered, the tunnel boring machine must be supplemented or replaced by the drill-blast method. Because of excessive cutter wear and unacceptable amounts of downtime, the boring machines also experience great difficulty in hard, abrasive rock formations, and the cyclic drill-blast procedures remain the only reliable, economic tunnel excavating method. Although many novel techniques employing plasma torches, lasers, hydraulic jets, and electron beam guns have been studied at near prototype scales, none have yet shown sufficient promise to warrant development into a full-scale, production-line tunneling machine for hard rock. Explosive fragmentation, despite its comparatively low efficiency in soft rock, will continue to be used to help tunnel boring machines during adverse conditions and often provides the only feasible method for excavation of tunnels and openings in hard rock. These facts demonstrate the need for a better understanding of problems inherent in using the drill-blast method for underground excavation.

Many problems of damage from underground blasting differ from those encountered in quarry blasting. Although the producing mine or tunnel operation normally does not have to be concerned with damage to residential structures, the shock and high-intensity waves from underground blasts may damage roof rock necessary to support the opening. The vibrations from the blast zone may affect roof bolt stability and damage mine support systems or other underground structures (19).[4] Excessively high airblast overpressures from underground blasts may damage mine ventilation walls (17). In addition, the increasing use of explosive fragmentation to excavate shallow underground openings in urban areas, and the possibility of using nuclear energy for mining operations emphasize the need to determine whether blasting recommendations found useful for quarry blasting may also be employed to design safe underground mine and tunnel rounds.

Prior to the Advisory Conference on Tunneling sponsored by the Organization for Economic Cooperation and Development (OECD) in Washington, D.C., June 22-26, 1970, representatives from all phases of the world's tunneling industry were questioned about needed improvements in tunneling technology. The spectrum of interest ranged from problems in excavating muds and soft strata for urban transportation and sanitary projects to blasting tunnels in hard rock. Almost every country indicated the importance of improving

[4]Underlined numbers in parentheses refer to items in the list of references at the end of this report.

explosive fragmentation techniques (7). Controlling damage to nearby structures and the surrounding rock from air and ground disturbances produced by blasting received the greatest support among suggested techniques for improving the drill-blast method.

The Bureau has conducted several previous studies on the problems of damage from blast vibrations. A few of its early investigations had measured the vibrations of floors, pillars, and roofs of underground mines (6, 9, 20) but most of the field research on ground vibrations has been concentrated on the problem of damage to such surface structures as private residences from vibrations produced by quarry blasts (1-5, 10-12, 21). The results of the quarry blast vibration studies by the Bureau and other investigators have recently been summarized and interpreted by Nicholls, Johnson, and Duvall (11).

To estimate vibration levels from various charge sizes, a method of combining the vibration data from the different quarries was needed. One of the most important findings of the Bureau's quarry vibration studies was that although each site had a different scaling factor which best grouped the data, scaling (dividing) the distance by the square root of the charge weight per delay was empirically shown to remove the effect of charge weight on the amplitude of peak particle velocity (11). Although other investigators have suggested that cube root scaling, determined from dimensional analysis, should be used, the Bureau found that cube root scaling did not reduce the spread of the quarry blast vibration data as would be true had cube root scaling been more appropriate. This conclusion implies that blast design (specifically the charge length, diameter of holes, or number of holes) strongly influences the scaling.

As a result of vibration monitoring experiments in operating mines at White Pine, Mich., and Shullsburg, Wis. (14-16, 18), the Bureau found that maximum amplitudes of the high-intensity elastic waves associated with routine production blasts were produced by the charge weight fired in the zero delay interval. Although some contributions due to the wave additions from the caps with higher delay periods were observed at the more remote gage stations, the high-intensity portions of the waveforms of all the periods were separate events. Hence, reducing the zero-delay charge weight could effectively reduce the maximum vibration amplitudes of the blast. The intense vibration levels near the face were attenuated very rapidly as the waves traveled through the mine roof strata.

Statistical analysis of the roof vibration data from the blasts at the White Pine mine also demonstrated that scaling the distance by the square root of the charge weight provided better grouping of the vibration data than scaling by the cube root (15, 18). Data from the experiments at Shullsburg did not have a sufficiently large range of charge sizes to permit determination of a scaling factor, and hence these data were also scaled by the square root of the charge weight to compare the vibration levels with other published work (14, 16).

Because blast parameters, opening configuration, and gage placement could have a strong influence on the scaling factor, enough data from different

sites are needed to determine what scaling factor should be used to group vibration data from underground mine and tunnel blasts and to design safe blasting rounds.

## ACKNOWLEDGMENTS

The authors wish to acknowledge the cooperation of the U.S. Army Corps of Engineers and NORAD personnel in this test program. Larry R. Fletcher, engineering technician, and Dennis V. D'Andrea, geophysicist, Twin Cities Mining Research Center, assisted in the field work and helped reduce and prepare the data for this report.

## TEST SITE

The NORAD Complex is located at Cheyenne Mountain, El Paso County, Colo., 5 miles south of Colorado Springs (fig. 1). The underground complex houses the Combat Operation Center and the necessary support facilities such as a communications center, barracks, mess hall, infirmary, repair shops, and materiel storage. Three-story steel buildings, having a total floor space of 176,000 $ft^2$ (16 300 $m^2$)[5] are mounted on springs in three parallel underground chambers (fig. 2). The main chambers are 45 ft (14 m) wide, 60 ft (18 m) high, and 600 ft (180 m) long. Separated by rock pillars 100 ft (30 m) wide, these long chambers are connected by three intersecting chambers 32 ft (10 m) wide, 56 ft (17 m) high, spaced about 130 ft (40 m) apart. Utility facilities, including power generation, air conditioning, and fuel oil and water storage occupy excavations adjacent to the building area. The complex is capable of

[5]The prime units in the text, tables, and illustrations of this publication are the U.S. customary units. Where appropriate, the approximate equivalents in the International System of Units (SI) are either included or used alone in accordance with the rules for introducing modernized metric units established by the National Bureau of Standards ASTM Metric Practice Guide, Handbook 102. In accordance with the SI convention, a space rather than a comma is used to separate the digits in a metric number such as 15 000. The U.S. customary numbers used throughout the report include commas, where necessary, to separate the digits. The period is used as a decimal point in both SI and U.S. customary numbers.

Abbreviations

| U.S. customary units | SI units |
|---|---|
| in = inch | mm = millimeter |
| ft = foot | m = meter |
| lb = pound | kg = kilogram |
| mv = millivolt | N = newton |
| msec = millisecond | mv = millivolt |
| Hz = Hertz (unit of frequency--cycle per second) | msec = millisecond |
| | Hz = Hertz (unit of frequency--cycle per second) |
| | M = mega (prefix 1 000 000) |
| | G = giga (prefix 1 000 000 000) |

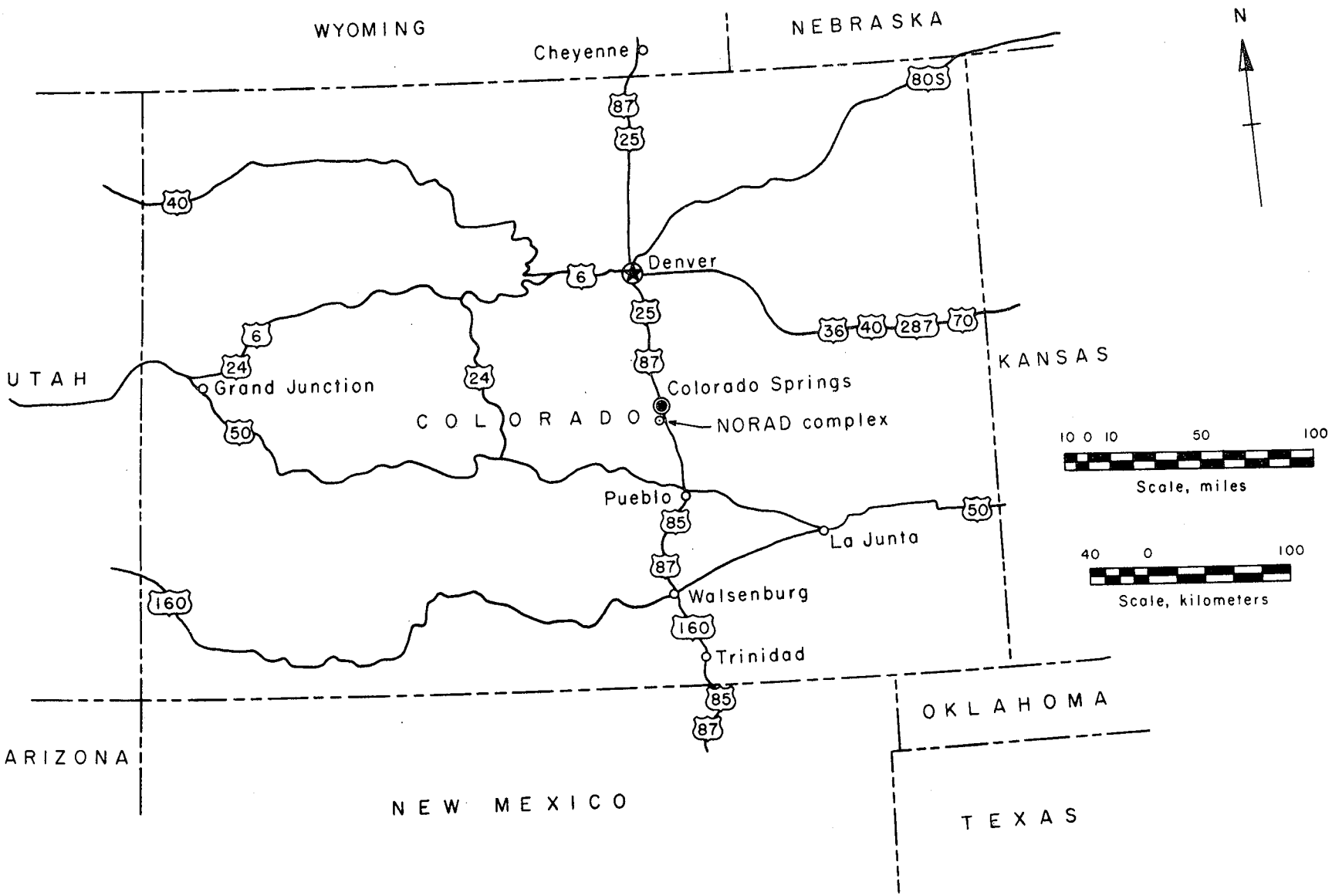


FIGURE 1. - Location of NORAD Complex, Cheyenne Mountain, Colo.

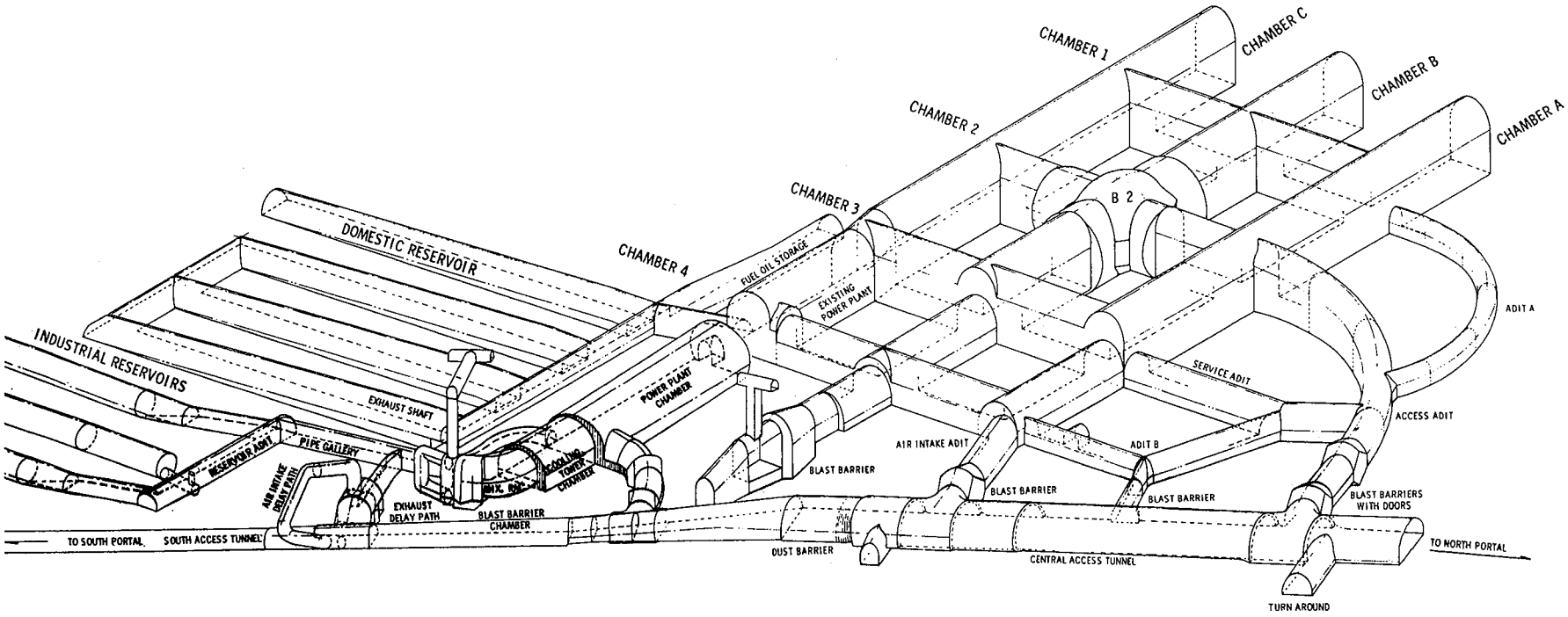


FIGURE 2. - General View of NORAD Complex.

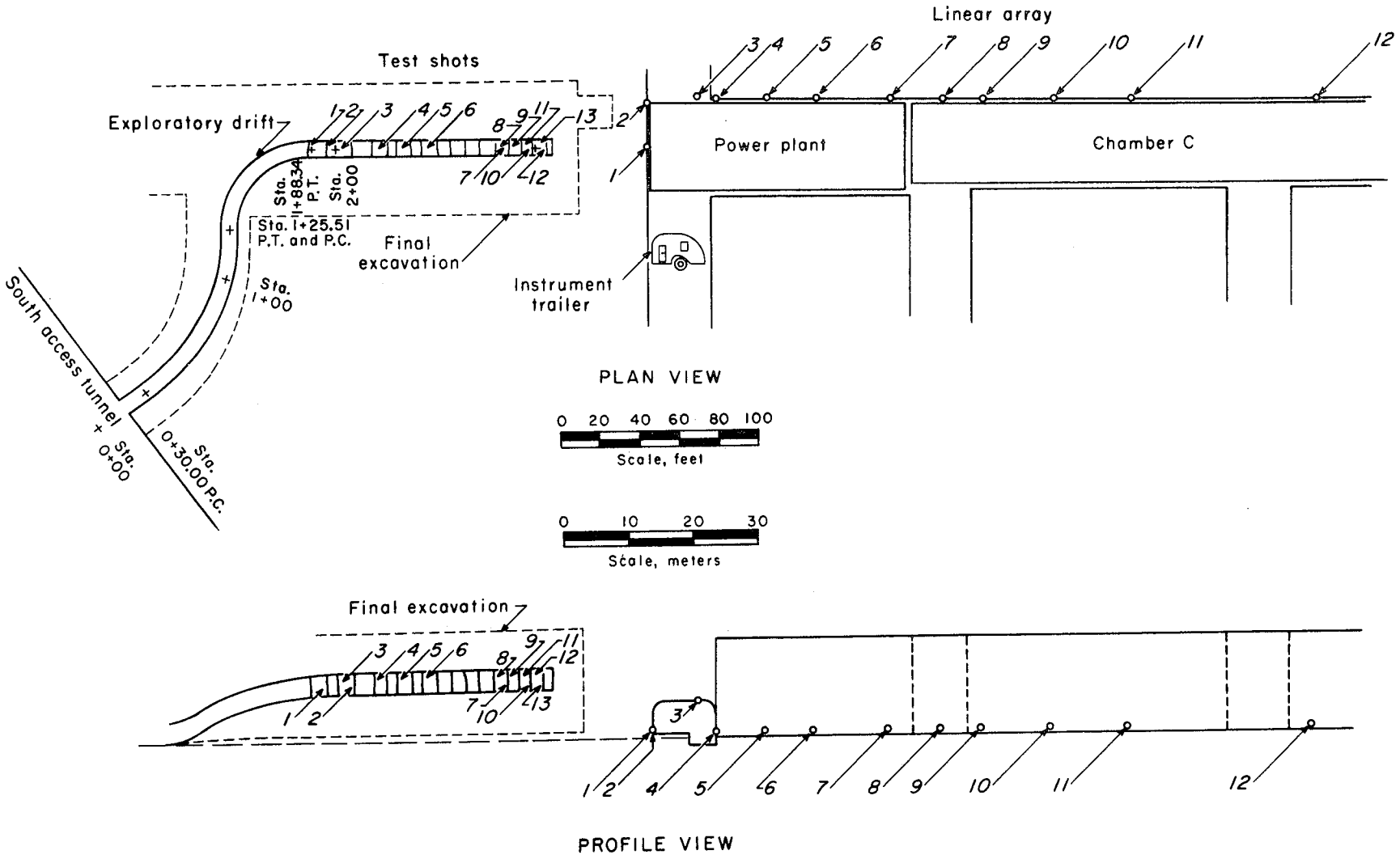


FIGURE 3. - Plan and Profile Views of Exploratory Drift and Gage Stations.

self-contained operation under closed-off status for an extended period of time in the event of an attack (8, 22). The proposed new construction (powerplant chamber, cooling tower chamber, and mix room) is shown by the shaded area in figure 2. The exploratory drift followed the curve from the south access tunnel into the side of the powerplant chamber and ran almost the entire length of the chamber toward the powerplant. Figure 3 shows the location of the exploratory drift and the gage locations for measuring the vibrations from the tunnel blasts in the exploratory drift.

The NORAD Complex was constructed in the Pikes Peak Granite of Precambrian age. The general geology of the site has been described by Ogden (13). The Corps of Engineers mapped the detailed geology of the exploratory drift as part of the planning for the NORAD Complex expansion project and observed that the rock around the exploratory drift is generally a coarse-grained biotite granite intruded by a fine-to-medium-grained granite. The rock is essentially fresh and unaltered except for some thin zones. Fractures in the rock mass are moderately to closely spaced. At station 0+20 (fig. 3), a small mass of fine-to-medium-grained granite was observed, and a large mass of similar rock extends from station 2+30 to 3+00. The granite at these locations is also essentially fresh and unaltered with closely spaced fractures. The effects of the rock texture and structural defects are reflected in the physical properties of the coarse-grained Pikes Peak Granite. Table 1 shows the results of the acoustic tests and the calculated values for dynamic Young's modulus, dynamic shear modulus, and Poisson's ratio for the four cores obtained from the exploratory drift. Tables 2 and 3 give the tensile and compressive strength measurements. In general, the tests indicate that this section of the Pikes Peak Granite is a less competent rock than would be expected.

TABLE 1. - Acoustic tests of NORAD granite samples[1]

| Sample No. | Length, mm | Diameter, mm | Longitudinal pulse velocity, m/sec | Longitudinal bar velocity, m/sec | Torsional velocity, m/sec | Dynamic Young's modulus, $GN/m^2$ | Dynamic Young's modulus, $10^6$ $lb/in^2$ | Dynamic shear modulus, $GN/m^2$ | Dynamic shear modulus, $10^6$ $lb/in^2$ | Poisson's ratio[2] |
|---|---|---|---|---|---|---|---|---|---|---|
| 1707 | 151.66 | 47.32 | 3,740 | 3,123 | 2,392 | 26.6 | 3.85 | 15.6 | 2.26 | 0.322 |
| 1708 | 154.86 | 47.31 | 4,170 | 3,544 | 2,411 | 34.1 | 4.94 | 15.8 | 2.29 | .311 |
| 1709 | 154.86 | 47.27 | 3,810 | 3,503 | 2,481 | 33.5 | 4.86 | 16.8 | 2.44 | .245 |
| 1710 | 168.35 | 52.25 | 4,270 | 3,119 | 2,143 | 25.5 | 3.69 | 12.0 | 1.74 | .381 |
| Mean | - | - | 4,006 | 3,323 | 2,357 | 29.9 | 4.34 | 15.0 | 2.18 | .315 |
| $\sigma$ | - | - | 261 | 233 | 148 | 4.52 | .656 | 2.09 | .303 | .056 |

[1]Rock property measurements were performed by the Property Determination Research Support group of this center.

[2]Derived from ratio of longitudinal bar velocity to longitudinal pulse velocity.

TABLE 2. - Tensile strength tests of NORAD granite samples[1]

| Sample No. | Diameter, mm | Tensile strength, $MN/m^2$ | Tensile strength, $lb/in^2$ |
|---|---|---|---|
| 1707 | 47.35 | 3.32 | 482 |
| 1708 | 47.38 | 2.88 | 417 |
| 1709 | 47.37 | 3.97 | 575 |
| 1710 | 52.25 | 1.45 | 210 |
| Mean | - | 2.91 | 421 |
| $\sigma$ | - | 1.07 | 155 |

[1]Rock property measurements were performed by the Property Determination Research Support group of this center.

TABLE 3. - Compressive strength tests of NORAD granite samples[1]

| Sample No. | Length, mm | Diameter, mm | Young's modulus, $GM/m^2$ | Young's modulus, $10^6$ lb/in$^2$ | Compressive strength, $MN/m^2$ | Compressive strength, $10^3$ lb/in$^2$ |
|---|---|---|---|---|---|---|
| 1707 | 73.18 | 47.36 | 31.2 | 4.52 | 117 | 17.0 |
| 1708 | 76.05 | 47.34 | 39.9 | 5.78 | 139 | 20.1 |
| 1709 | 74.89 | 47.35 | 38.6 | 5.60 | 150 | 21.7 |
| 1710 | 83.26 | 52.24 | 29.3 | 4.25 | 69 | 10.1 |
| Mean | - | - | 34.7 | 5.04 | 119 | 17.2 |
| $\sigma$ | - | - | 5.29 | .767 | 35.6 | 5.17 |

[1]Rock property measurements were performed by the Property Determination Research Support group of this center.

Results of earlier tests on cores from other zones of the coarse-grained granite from the NORAD site indicated a compressive strength for unaltered rock of 20,000 lb/in$^2$ (138 $MN/m^2$) and 10,000 lb/in$^2$ (69 $MN/m^2$) for altered rock (22). Tensile strength of the unaltered rock was about 1,300 lb/in$^2$ (9 $MN/m^2$).

## EXPERIMENTAL PROCEDURE

### Instrumentation

The recording instrumentation consisted of two separate systems with a total capacity of 28 information channels. System No. 1 consisted of particle velocity gages with a reasonably flat response from 10 to 500 Hz, voltage amplifiers (dc--15,000 Hz ±3 percent), and a 14-channel FM magnetic tape recorder. Voltage amplifier outputs were recorded on the tape recorder at a speed of 60 in/sec (approximately 1 524 mm/sec). Recorded shots were replayed at a speed of 1-7/8 in/sec (approximately 47.6 mm/sec) to either an oscilloscope or a direct-writing oscillograph.

System No. 2 employed similar particle velocity gages but different type voltage amplifiers (2 to 10,000 Hz ±3 percent). The outputs of these voltage amplifiers were fed directly to a 14-channel, direct-writing oscillograph.

Individual components of the recording systems were calibrated before each field trip. Particle velocity gages were calibrated on a shake table. In the field, each channel was calibrated before every shot by a standard calibration signal. When the data were analyzed, comparison of the unknown amplitude on the record and the recorded calibration signal gave the indicated particle velocity.

An array of 12 gages was placed along the rock walls in chamber C (fig. 3) to record the vibration amplitude as a function of charge weight and distance from the blast. Two gages were placed at the front end of the powerplant chamber: one at the center of the building and one near the corner. The remaining 10 gages were positioned in a linear array at distances ranging from 25 to 338 ft (7.6 to 103 m) from the front end of the chamber. These gages

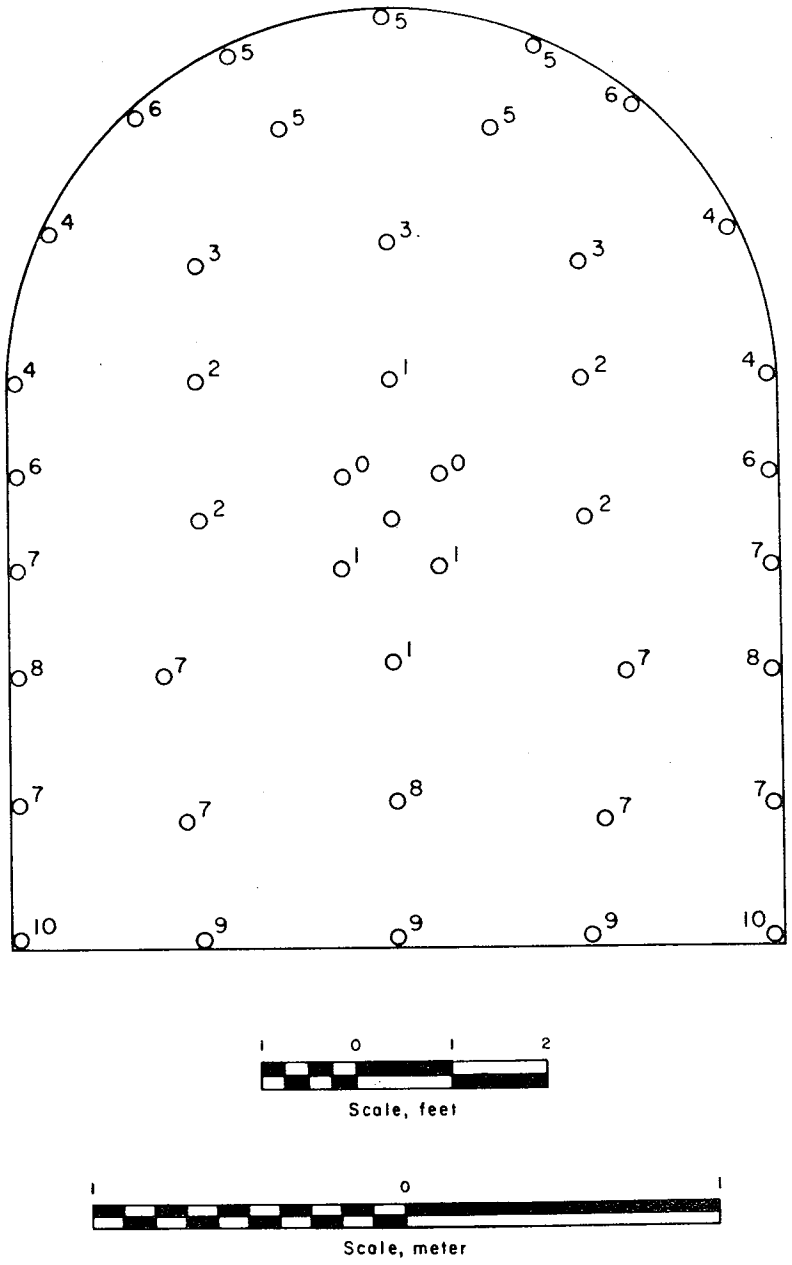


FIGURE 4. - NORAD Blast Round.

were mounted on 1/2-in- (13-mm) thick aluminum plates, epoxied to the rock and oriented to measure vertical particle velocity. Gages 1 and 2 at the front end of the chamber were considered as part of the linear array in the data analysis.

## Blasting Operations

The blast rounds contained from 41 to 47 blastholes with a five-hole burn cut near the center of the drift. A typical blast round is shown in figure 4. The hole in the center of the pattern was not loaded and served as the free face for the zero-delay holes in opening the cut. The blastholes were drilled to a depth of 7 to 8 ft (2.1 to 2.4 m), with a 1-1/4- (32-mm) or 1-1/2-in (38-mm) tungsten carbide insert bit and an air-leg mounted percussive drill. The rounds were drilled to pull an opening at least 8 ft (2.4 m) wide and 10 ft (3.0 m) high, as shown in the figure. Eleven periods of slow tunnel delay electric blasting caps were used. Table 4 shows the average delay time of each period.

The shots were fired electrically from a station at the portal of the south access tunnel. When a shot was to be recorded, a telephone countdown system was used to assure that the recording system was operating at the proper speed at the time of the blast.

The powder charge per hole was varied from 3 to 6 lb (1.4 to 2.7 kg), depending on the location of the hole and the type of explosive.

TABLE 4. - Delay times of tunnel delays used at NORAD

| Delay No. | Average delay time, sec |
|---|---|
| 0 | 0.008 |
| 1 | .025 |
| 2 | .30 |
| 3 | .50 |
| 4 | .75 |
| 5 | 1.00 |
| 6 | 1.50 |
| 7 | 2.00 |
| 8 | 2.50 |
| 9 | 3.00 |
| 10 | 3.50 |

The explosives used in driving the exploratory drift included various combinations of Gelamite[6] 2, a 45-percent semigelatin, Hercon 2, a 50-percent low-density ammonia dynamite, and air-emplaced ammonium nitrate prills and fuel oil (AN-FO). Table 5 gives the properties of the explosives used for the NORAD experiment.

TABLE 5. - Properties of explosives used for the NORAD experiment

| Property | Gelamite 2 | Hercon 2 | AN-FO[1] |
|---|---|---|---|
| Detonation velocity.....ft/sec.. | 11,500 | 11,500 | 9,500 |
| Do.....m/sec.. | 3 500 | 3 500 | 2 900 |
| Specific gravity..... | 1.2 | 1.2 | 0.95 |
| Calculated detonation pressure.....kbars.. | 34 | 34 | 21 |
| Do.....$10^6$ N/m$^2$.. | 3.4 | 3.4 | 2.1 |
| Water resistance..... | Good | Fair | Very poor |
| Fume class..... | Good | Good | Good |

[1]Assuming air injection into a 1-1/2-in (38-mm) borehole.

Because caps with higher delay periods have considerable scatter in firing times and the exact amount of explosive detonating at a given time within a period is indeterminable, instantaneous or zero-delay blasting caps must be used to provide meaningful vibration measurements from tunnel blasts of various sizes. If the normal blast rounds were used, only vibrations from the very small charge weights fired with the zero delay could be obtained to generate the empirical propagation equation.

To measure ground vibrations from larger charge weights, special shots using zero-delay caps were fired (table 6).

[6]Reference to specific trade names is made for identification only and does not imply endorsement by the Bureau of Mines.

TABLE 6. - Description of test rounds

| Shot No. | Description | No. of holes | Charge weight | | Explosive type |
|---|---|---|---|---|---|
| | | | Lb | Kg | |
| 1 | 0-delay portion of burn cut. | 2 | 6.8 | 3.1 | Gelamite 2. |
| 2 | .....do..... | 2 | 6.8 | 3.1 | Do. |
| 3 | Perimeter holes fired with instantaneous caps. | 12 | 36.6 | 16.6 | Do. |
| 4 | 0-delay portion of burn cut. | 2 | 7.5 | 3.4 | Do. |
| 5 | .....do..... | 1 | 3.7 | 1.7 | Do. |
| 6 | .....do..... | 3 | 11.2 | 5.1 | Do. |
| 7 | .....do..... | 1 | 3.4 | 1.5 | Hercon 2. |
| 8 | Perimeter holes from shot No. 7 fired instantaneously. | 4 | 15.1 | 6.8 | Do. |
| 9 | Perimeter holes fired instantaneously. | 6 | 19.7 | 9.0 | Do. |
| 10 | Crater cut at center of face, fired instantaneously. | 6 | 18.7 | 8.5 | Do. |
| 11 | Perimeter holes fired instantaneously. | 14 | 47.0 | 21.4 | Do. |
| 12 | 0-delay portion of burn cut. | 1 | 4.1 | 1.9 | Gelamite 2. |
| 13 | Perimeter holes fired with instantaneous caps and Primacord. | 17 | 73.4 | 33.3 | Hercon 2--56.7 lb (25.7 kg). Gelamite 2--16.7 lb (7.6 kg). |

## EXPERIMENTAL DATA

Vibration records of particle velocity as a function of time were obtained for the 13 blasts described in table 6. Typical records are shown in figure 5. The record for shot No. 4 (7.5 lb (3.4 kg)) represents the vertical component of the vibrations recorded at gage station No. 3 for the zero-delay portion of the burn cut. The illustrated vibration record from shot No. 13 (73.4 lb (33.3 kg)) was also obtained at station No. 3 and was produced by the instantaneous detonation of the perimeter holes.

Most of the normal tunnel blast rounds included up to 11 periods of slow delays. Because the time interval between successive delays was long enough that the holes fired by the later delay periods produced separate bursts of vibrations later on the record, the charge weight fired by the zero-delay caps and not the total charge weight of the blasting round was used in all calculations.

Maximum peak particle velocity for each gage station was measured regardless of frequency or where it occurred on the record. The frequency of the pulse associated with the maximum peak particle velocity was also determined.

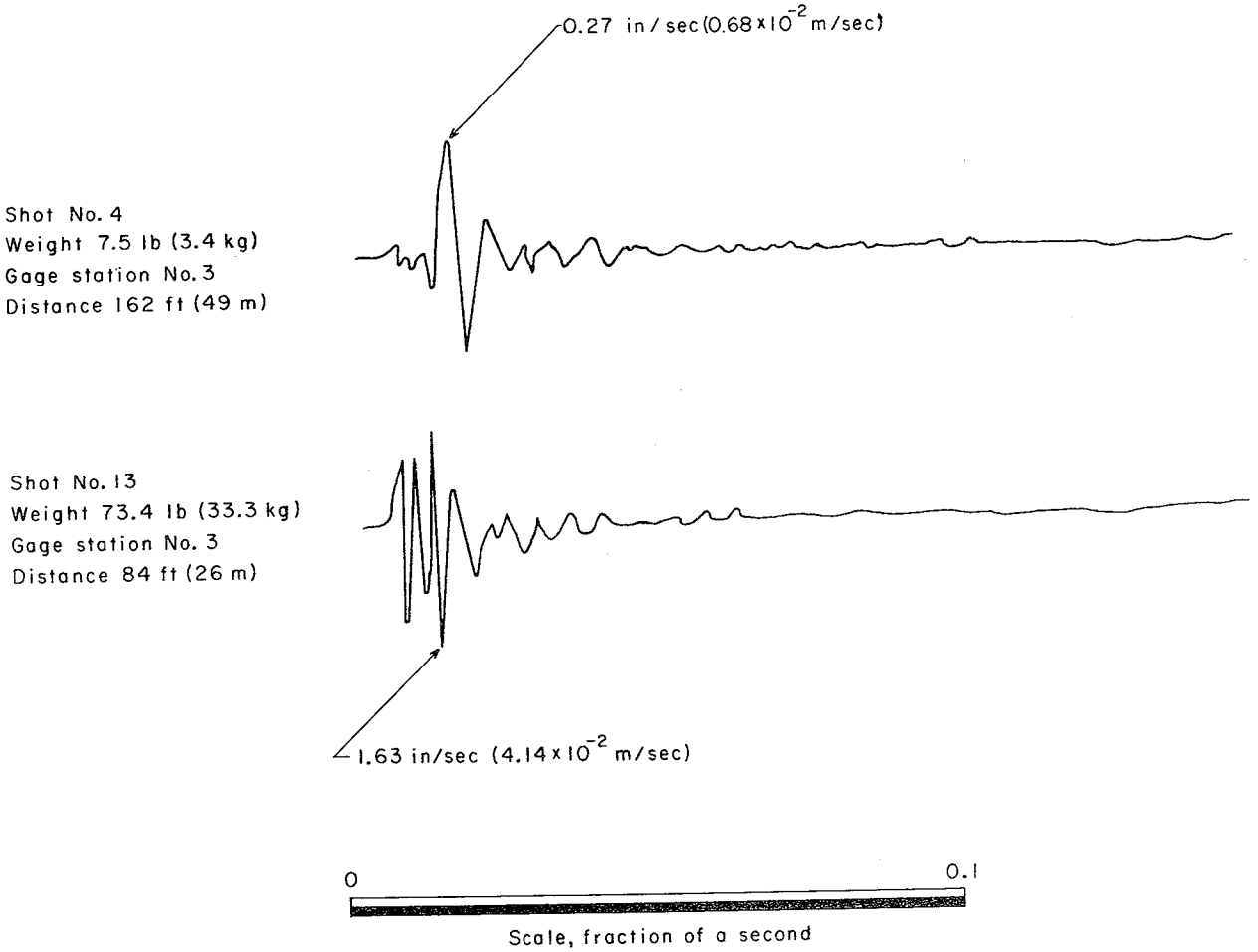


FIGURE 5. - Typical Vibration Records.

Table 7 contains the measured particle velocities and frequencies for the linear array gage stations, 1 through 12. Particle velocities for the linear array stations ranged from 0.003 to 2.2 in/sec ($0.008 \times 10^{-2}$ to $5.6 \times 10^{-2}$ m/sec), and frequencies ranged from 90 to 640 Hz.

TABLE 7. - NORAD particle velocity data

| Distance | | Scaled distance | | Maximum peak particle velocity | | Frequency of maximum velocity |
|---|---|---|---|---|---|---|
| Ft | m | $Ft/lb^{1/3}$ | $m/kg^{1/3}$ | In/sec | $10^{-2}$ m/sec | Hz |
| SHOT NO. 1 CHARGE WEIGHT 6.8 LB (3.1 kg) | | | | | | |
| 167 | 51 | 88.3 | 35.0 | 0.084 | 0.21 | 270 |
| 169 | 52 | 89.4 | 35.5 | .065 | .17 | 270 |
| 192 | 59 | 102 | 40.5 | .10 | .25 | 270 |
| 211 | 64 | 112 | 44.4 | .031 | .079 | 400 |
| 231 | 70 | 122 | 48.4 | .016 | .041 | 230 |
| 253 | 77 | 134 | 53.2 | .0063 | .016 | 230 |
| 290 | 88 | 153 | 60.7 | .016 | .041 | 270 |
| 316 | 96 | 167 | 66.2 | .010 | .025 | 230 |
| 337 | 103 | 178 | 70.6 | .0093 | .024 | 230 |

TABLE 7. - NORAD particle velocity data--Continued

| Distance | | Scaled distance | | Maximum peak particle velocity | | Frequency of maximum velocity, Hz |
|---|---|---|---|---|---|---|
| Ft | m | $Ft/lb^{1/3}$ | $m/kg^{1/3}$ | In/sec | $10^{-2}$ m/sec | |
| SHOT NO. 1 CHARGE WEIGHT 6.8 LB (3.1 kg)--Continued | | | | | | |
| 372 | 113 | 197 | 78.2 | 0.011 | 0.028 | 540 |
| 410 | 125 | 217 | 86.1 | .0047 | .012 | 230 |
| 504 | 154 | 267 | 106 | .0047 | .012 | 200 |
| SHOT NO. 2 CHARGE WEIGHT 6.8 LB (3.1 kg) | | | | | | |
| 199 | 61 | 105 | 41.7 | 0.058 | 0.15 | 160 |
| 218 | 66 | 115 | 45.6 | .050 | .13 | 160 |
| 241 | 74 | 128 | 50.8 | .034 | .086 | 180 |
| 277 | 84 | 147 | 58.3 | .048 | .12 | 160 |
| 304 | 93 | 161 | 63.9 | .028 | .071 | 160 |
| 325 | 99 | 172 | 68.2 | .023 | .058 | 150 |
| 360 | 110 | 190 | 75.4 | .028 | .071 | 130 |
| 398 | 121 | 211 | 83.8 | .017 | .043 | 110 |
| 492 | 150 | 260 | 103 | .015 | .038 | 110 |
| SHOT NO. 3 CHARGE WEIGHT 36.6 LB (16.6 kg) | | | | | | |
| 154 | 47 | 46.3 | 18.4 | 0.65 | 1.65 | 200 |
| 156 | 48 | 46.9 | 18.6 | .29 | .74 | 180 |
| 179 | 55 | 53.9 | 21.4 | .52 | 1.32 | 200 |
| 199 | 61 | 59.9 | 23.8 | .15 | .38 | 260 |
| 218 | 66 | 65.6 | 26.0 | .069 | .18 | 160 |
| 241 | 74 | 72.5 | 28.8 | .073 | .19 | 230 |
| 277 | 84 | 83.4 | 33.1 | .071 | .18 | 180 |
| 304 | 93 | 91.5 | 36.3 | .046 | .12 | 230 |
| 325 | 99 | 97.8 | 38.8 | .041 | .10 | 230 |
| 360 | 110 | 108 | 42.8 | .052 | .13 | 200 |
| 398 | 121 | 120 | 47.6 | .028 | .071 | 180 |
| 492 | 150 | 148 | 58.7 | .014 | .036 | 150 |
| SHOT NO. 4 CHARGE WEIGHT 7.5 LB (3.4 kg) | | | | | | |
| 137 | 42 | 69.8 | 27.7 | 0.34 | 0.86 | 200 |
| 139 | 42 | 70.9 | 28.1 | .19 | .48 | 230 |
| 162 | 49 | 82.6 | 32.8 | .27 | .68 | 180 |
| 182 | 56 | 92.8 | 36.8 | .074 | .19 | 270 |
| 201 | 61 | 103 | 40.9 | .054 | .14 | 270 |
| 224 | 68 | 114 | 45.2 | .044 | .11 | 180 |
| 261 | 80 | 133 | 52.8 | .054 | .14 | 200 |
| 287 | 88 | 146 | 58.0 | .031 | .079 | 180 |
| 308 | 94 | 157 | 62.3 | .031 | .079 | 160 |
| 343 | 105 | 175 | 69.4 | .026 | .066 | 160 |
| 381 | 116 | 194 | 77.0 | .012 | .030 | 200 |
| 475 | 145 | 242 | 96.0 | .012 | .030 | 110 |
| SHOT NO. 5 CHARGE WEIGHT 3.7 LB (1.7 kg) | | | | | | |
| 125 | 38 | 80.6 | 32.0 | 0.20 | 0.51 | 230 |
| 127 | 39 | 81.9 | 32.5 | .15 | .38 | 270 |
| 150 | 46 | 96.7 | 38.4 | .069 | .18 | 160 |
| 170 | 52 | 110 | 43.6 | .047 | .12 | 300 |
| 190 | 58 | 123 | 48.8 | .046 | .12 | 270 |

TABLE 7. - NORAD particle velocity data--Continued

| Distance | | Scaled distance | | Maximum peak particle velocity | | Frequency of maximum velocity, Hz |
|---|---|---|---|---|---|---|
| Ft | m | $Ft/lb^{1}/^{3}$ | $m/kg^{1}/^{3}$ | In/sec | $10^{-2}$ m/sec | |
| SHOT NO. 5 CHARGE WEIGHT 3.7 LB (1.7 kg)--Continued | | | | | | |
| 212 | 65 | 137 | 54.3 | 0.020 | 0.051 | 110 |
| 249 | 76 | 161 | 63.9 | .029 | .074 | 180 |
| 275 | 84 | 177 | 70.2 | .013 | .033 | 180 |
| 296 | 90 | 191 | 75.8 | .0085 | .022 | 200 |
| 331 | 101 | 214 | 85.0 | .0077 | .020 | 200 |
| 369 | 113 | 238 | 94.4 | .0050 | .013 | 150 |
| 463 | 141 | 299 | 119 | .0039 | .010 | 120 |
| SHOT NO. 6 CHARGE WEIGHT 11.2 LB (5.1 kg) | | | | | | |
| 112 | 34 | 50.0 | 19.8 | 0.40 | 1.02 | 230 |
| 114 | 35 | 50.8 | 20.2 | .35 | .89 | 270 |
| 137 | 42 | 61.1 | 24.2 | .40 | 1.02 | 230 |
| 158 | 48 | 70.5 | 28.0 | .12 | .30 | 320 |
| 177 | 54 | 79.0 | 31.3 | .066 | .17 | 400 |
| 199 | 61 | 88.8 | 35.2 | .044 | .11 | 320 |
| SHOT NO. 7 CHARGE WEIGHT 3.4 LB (1.5 kg) | | | | | | |
| 77 | 23 | 51.3 | 20.4 | 0.51 | 1.30 | 640 |
| 102 | 31 | 68.0 | 27.0 | .23 | .58 | 370 |
| 142 | 43 | 94.6 | 37.6 | .070 | .18 | 340 |
| 201 | 61 | 134 | 53.2 | .033 | .084 | 230 |
| 248 | 76 | 165 | 65.5 | .021 | .053 | 310 |
| 321 | 98 | 214 | 84.9 | .0081 | .021 | 210 |
| SHOT NO. 8 CHARGE WEIGHT 15.1 LB (6.8 kg) | | | | | | |
| 77 | 23 | 31.1 | 12.3 | 0.41 | 1.04 | 540 |
| 102 | 31 | 41.2 | 16.3 | .23 | .58 | 270 |
| 142 | 43 | 57.4 | 22.8 | .11 | .28 | 400 |
| 201 | 61 | 81.3 | 32.3 | .058 | .15 | 160 |
| 248 | 76 | 100 | 39.7 | .034 | .086 | 130 |
| 321 | 98 | 130 | 51.6 | .016 | .041 | 100 |
| SHOT NO. 9 CHARGE WEIGHT 19.7 LB (9.0 kg) | | | | | | |
| 71 | 22 | 26.2 | 10.4 | 0.68 | 1.73 | 320 |
| 96 | 29 | 35.5 | 14.1 | .34 | .86 | 230 |
| 136 | 41 | 50.3 | 20.0 | .10 | .25 | 320 |
| 195 | 59 | 72.2 | 28.6 | .12 | .30 | 140 |
| 242 | 74 | 89.6 | 35.5 | .042 | .11 | 200 |
| 315 | 96 | 117 | 46.4 | .025 | .063 | 140 |
| SHOT NO. 10 CHARGE WEIGHT 18.7 LB (8.5 kg) | | | | | | |
| 66 | 20 | 24.9 | 9.88 | 0.17 | 0.43 | 320 |
| 69 | 21 | 26.0 | 10.3 | .32 | .81 | 320 |
| 90 | 27 | 33.9 | 13.4 | .33 | .84 | 230 |
| 113 | 34 | 42.6 | 16.9 | .21 | .53 | 320 |
| 130 | 40 | 49.0 | 19.4 | .10 | .25 | 400 |
| 152 | 46 | 57.3 | 22.7 | .083 | .21 | 160 |
| 189 | 58 | 71.3 | 28.3 | .048 | .12 | 290 |
| 215 | 66 | 81.1 | 32.2 | .052 | .13 | 320 |
| 236 | 72 | 89.0 | 35.3 | .045 | .11 | 290 |

TABLE 7. - NORAD particle velocity data--Continued

| Distance | | Scaled distance | | Maximum peak particle velocity | | Frequency of maximum velocity, Hz |
|---|---|---|---|---|---|---|
| Ft | m | $Ft/lb^{1/3}$ | $m/kg^{1/3}$ | In/sec | $10^{-2}$ m/sec | |
| SHOT NO. 10 CHARGE WEIGHT 18.7 LB (8.5 kg)--Continued | | | | | | |
| 271 | 83 | 102 | 40.5 | 0.036 | 0.091 | 110 |
| 309 | 94 | 117 | 46.4 | .014 | .036 | 90 |
| 403 | 123 | 151 | 59.9 | .0089 | .023 | 130 |
| SHOT NO. 11 CHARGE WEIGHT 47.0 LB (21.4 kg) | | | | | | |
| 66 | 20 | 18.2 | 7.22 | 1.00 | 2.54 | 160 |
| 69 | 21 | 19.1 | 7.58 | 1.42 | 3.61 | 230 |
| 90 | 27 | 24.9 | 9.88 | .66 | 1.68 | 320 |
| 113 | 34 | 31.3 | 12.4 | .42 | 1.07 | 270 |
| 130 | 40 | 36.0 | 14.3 | .29 | .74 | 200 |
| 152 | 46 | 42.1 | 16.7 | .22 | .56 | 160 |
| 189 | 58 | 52.3 | 20.7 | .15 | .38 | 150 |
| 215 | 66 | 59.5 | 23.6 | .15 | .38 | 140 |
| 236 | 72 | 65.3 | 25.9 | .059 | .15 | 140 |
| 271 | 83 | 75.0 | 29.8 | .087 | .22 | 120 |
| 309 | 94 | 85.5 | 33.9 | .035 | .089 | 110 |
| 403 | 123 | 112 | 44.4 | .023 | .058 | 130 |
| SHOT NO. 12 CHARGE WEIGHT 4.1 LB (1.9 kg) | | | | | | |
| 60 | 18 | 37.5 | 14.9 | 0.19 | 0.48 | 400 |
| 64 | 20 | 40.0 | 15.9 | .20 | .51 | 540 |
| 84 | 26 | 52.5 | 20.8 | .17 | .43 | 400 |
| 107 | 33 | 66.4 | 26.3 | .12 | .30 | 400 |
| 124 | 38 | 77.5 | 30.7 | .047 | .12 | 400 |
| 146 | 45 | 91.2 | 36.2 | .039 | .099 | 320 |
| 183 | 56 | 114 | 45.2 | .023 | .058 | 320 |
| 209 | 64 | 131 | 52.0 | .011 | .028 | 260 |
| 230 | 70 | 144 | 57.1 | .013 | .033 | 320 |
| 265 | 81 | 166 | 65.9 | .019 | .048 | 400 |
| 303 | 92 | 189 | 75.0 | .0045 | .011 | 200 |
| 397 | 121 | 248 | 98.4 | .0034 | .0086 | 270 |
| SHOT NO. 13 CHARGE WEIGHT 73.4 LB (33.3 kg) | | | | | | |
| 60 | 18 | 14.3 | 5.67 | 2.20 | 5.59 | 230 |
| 64 | 20 | 15.3 | 6.07 | 2.23 | 5.66 | 200 |
| 84 | 26 | 20.0 | 7.93 | 1.63 | 4.14 | 320 |
| 107 | 33 | 25.5 | 10.1 | 1.18 | 3.00 | 230 |
| 124 | 38 | 29.6 | 11.7 | .48 | 1.22 | 200 |
| 146 | 45 | 34.9 | 13.8 | .51 | 1.30 | 130 |
| 183 | 56 | 43.7 | 17.3 | .31 | .79 | 150 |
| 209 | 64 | 50.0 | 19.8 | .35 | .89 | 130 |
| 230 | 70 | 55.0 | 21.8 | .17 | .43 | 90 |
| 265 | 81 | 63.3 | 25.1 | .22 | .56 | 120 |
| 303 | 92 | 72.4 | 28.7 | .11 | .28 | 100 |
| 397 | 121 | 94.9 | 37.6 | .063 | .16 | 100 |

## ANALYSIS OF DATA AND DISCUSSION

Through study of ground vibrations from quarry blasts (11) the Bureau has determined that the peak particle velocity V of each component of ground motion can be related to distance D and charge weight per delay W by an equation of the form

$$V = K \left( \frac{D}{W^b} \right)^{-n}, \tag{1}$$

where the unknown coefficients are K, the velocity intercept at unit scaled distance; b, the scaling exponent; and n, the decay exponent. The effect of the charge weight on the amplitude of the peak particle velocity data from the quarry blasts was removed by scaling the distance by the square root of the charge weight (that is, b = 1/2). Although cube-root scaling is supported by dimensional analysis, the Bureau has found no reduction in the spread of the quarry blast data when cube-root scaling was used. Square-root scaling is therefore recommended for designing safe quarry blasts.

The Bureau experiments at White Pine (15, 18) also demonstrated that square-root rather than cube-root scaling was appropriate for removing the effect of varying charge weight of mine production blasts.

Because the geometrical configurations for the openings and the blast rounds for the NORAD tests were significantly different from those at either White Pine or Shullsburg, the Bureau performed a statistical analysis on the NORAD vibration data to determine whether square-root or cube-root scaling would be an effective way to remove the effect of the charge weight on the peak particle velocity.

Another way of stating the relationship in equation 1 is that V is a ran dom variable whose theoretical value is given by equation 1. Equation 1 can also be written in the linear form

$$y_o = A + B \log D + C \log W, \tag{2}$$

where A = log K, B = -n, C = bn, and Y = log V is a random variable deviating from $y_o$ by an error term.

The usual assumptions used in analysis of variance are that Y is normall distributed within the ranges of expectation given by $y_o$ in equation 2, that constant variance exists independent of the distance and the shot, and that the sample values are independently distributed. The original observations V obviously had variances that increased with the mean. However, the log trans formation Y stabilizes these variances.

The following hypotheses were considered in the analysis. The indices i and j denote the $j^{th}$ measurement of (D, W, V) for the $i^{th}$ shot where $i = 1, \ldots, 13$, $j = 1, \ldots J(i)$, and $J(i)$ is the number of data points for shot i.

$$G : Y_{ij} = A + B \log D_{ij} + C \log W_i$$

$$H_1 : Y_{ij} = A + B (\log D_{ij} - 1/3 \log W_i)$$

$$H_2 : Y_{ij} = A + B (\log D_{ij} - 1/2 \log W_i).$$

Hypotheses $H_1$ and $H_2$ were tested against the alternative G to determine whether the data could be scaled by either of the exponents 1/3 or 1/2. The value of $F_{1,126}$ for testing $H_1$ against G was 1.15. The value of $F_{1,126}$ for testing $H_2$ against G was 34.95, which is statistically very significant, demonstrating that the scaling exponent b = 1/3 fits the data well, whereas the scaling exponent b = 1/2 does not adequately fit the data. The usual analysis of variance for these hypotheses is given in table 8. The error sum of squares is calculated from the general hypothesis G.

TABLE 8. - Analysis of variance

| Source | Sum of squares | Degrees of freedom | Mean square | F-ratio |
|---|---|---|---|---|
| $H_1$ ..... | 0.063 | 1 | 0.063 | 1.15 |
| $H_2$ ..... | 1.908 | 1 | 1.908 | 34.95 |
| Error..... | 6.877 | 126 | .055 | - |

The estimated values of the coefficients and their least-squares standard errors are listed in tables 9 and 10.

TABLE 9. - Estimated values of coefficients

| Hypothesis | A | B | C |
|---|---|---|---|
| $H_1$ ..... | 2.750 | -2.041 | - |
| $H_2$ ..... | 1.795 | -1.708 | - |
| G..... | 2.936 | -2.100 | 0.635 |

TABLE 10. - Least-squares standard errors of coefficients[1]

| Hypothesis | Standard error of B | Standard error of C | Standard error of y |
|---|---|---|---|
| $H_1$ ..... | 0.071 | - | 0.234 |
| $H_2$ ..... | .068 | - | .263 |
| G..... | .090 | 0.048 | .234 |

[1]Covariance between B and C under G = 0.035.

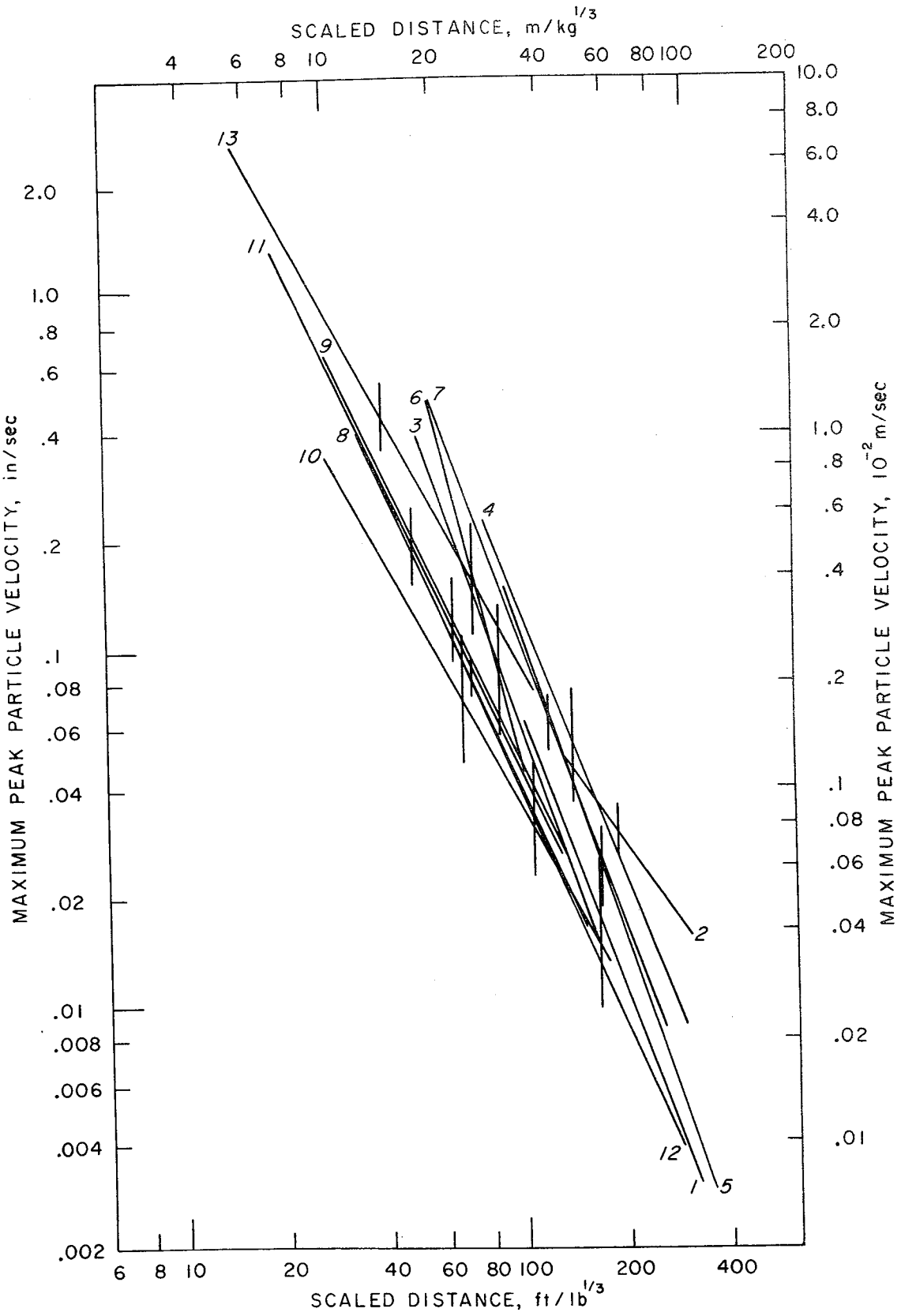


FIGURE 6. - Individual Least-Squares Regression Lines–NORAD Shots 1-13.

An approximate confidence interval for the scaling exponent b can be obtained by using the asymptotic distribution of

$$\hat{b} = -\frac{\hat{C}}{\hat{B}},$$

where $\hat{B}$ and $\hat{C}$ are the least-squares estimates of B and C under hypothesis G.

Let $\Sigma = \begin{pmatrix} \sigma_{11} & \sigma_{12} \\ \sigma_{21} & \sigma_{22} \end{pmatrix}$ be the covariance matrix of $\begin{pmatrix} \hat{B} \\ \hat{C} \end{pmatrix}$. Then $\hat{b}$ is asymptotically normal with mean b and variance given by $(\nabla b)\,\Sigma(\nabla b)$, where $\nabla b$ is the gradient of b with respect to (B,C):

$$\nabla b = \begin{pmatrix} C/B^2 \\ -1/B \end{pmatrix} = \frac{1}{-B}\begin{pmatrix} b \\ 1 \end{pmatrix}.$$

Hence, denoting the variance of $\hat{b}$ by $\sigma_b^2$, we have

$$\sigma_b^2 = B^{-2}\,(b^2\sigma_{11} + 2b\sigma_{12} + \sigma_{22}).$$

The actual value of $\sigma_b^2$ can be estimated from the least-squares estimates of B, C, and $\Sigma$ under the hypotheses listed in tables 9 and 10. This estimated value was found to be $\hat{\sigma}_b = 0.0277$. A confidence interval with confidence coefficient $\alpha$ can be approximated by $\left(\hat{b} - \sigma_b x_\alpha,\ \hat{b} + \sigma_b x_\alpha\right)$ where $P\left(|Z| \le x_\alpha\right) = \alpha$, and Z is a standardized normally distributed random variable. Because $\hat{b} = 0.303$ and $x_{0.95} = 1.96$, a 95-percent confidence interval for b is $0.249 \le b \le 0.357$.

Because the analysis of variance had shown that cube-root scaling was more appropriate for grouping the vibrations from the NORAD blasts, all the data points were scaled by dividing the distance by the cube root of the charge weight. Figure 6 shows the least-squares regression lines representing the data from each of the 13 shots. The vertical bar through the midpoint of the regression line represents one standard deviation of the scaled data above and below the line. Table 11 contains the intercepts K and the slopes n for the individual regression lines.

Because an empirical propagation equation was needed to predict vibration amplitudes from the larger production blasts planned for expanding the exploratory drift into a chamber, the vibration data shown in figure 6 were combined. The equation for the least-squares line through the combined data is

$$V = 560\left(\frac{D}{W^{1/3}}\right)^{-2.04},$$

where D is the distance in feet, W is the charge weight per delay in pounds, and V is the peak particle velocity in inches per second. In SI units the equation becomes

$$V = 2.15\left(\frac{D}{W^{1/3}}\right)^{-2.04},$$

where D is the distance in meters, W is the charge weight in kilograms, and V is the peak particle velocity in meters per second. Figure 7 shows the least-squares line through the combined NORAD data from the 13 shots. The vertical bar through the midpoint of the regression line represents one standard deviation of the scaled data above and below the line.

TABLE 11. - Least-squares coefficients for the individual regression lines--NORAD shots 1-13

| Shot No. | Charge weight | | Intercept, K | | Slope, -n | Standard deviation[1] | Data points |
|---|---|---|---|---|---|---|---|
| | Lb | Kg | In/sec | $10^{-2}$ m/sec | | | |
| 1 | 6.8 | 3.1 | 11,000 | 28 000 | -2.69 | 0.231 | 12 |
| 2 | 6.8 | 3.1 | 62 | 160 | -1.50 | .082 | 9 |
| 3 | 36.6 | 16.6 | 28,000 | 71 000 | -2.91 | .185 | 12 |
| 4 | 7.5 | 3.4 | 15,000 | 38 000 | -2.60 | .157 | 12 |
| 5 | 3.7 | 1.7 | 70,000 | 180 000 | -2.98 | .119 | 12 |
| 6 | 11.2 | 5.1 | 2,500,000 | 6 400 000 | -3.96 | .155 | 6 |
| 7 | 3.4 | 1.5 | 33,000 | 84 000 | -2.82 | .060 | 6 |
| 8 | 15.1 | 6.8 | 870 | 2 200 | -2.21 | .041 | 6 |
| 9 | 19.7 | 9.0 | 610 | 1 500 | -2.11 | .149 | 6 |
| 10 | 18.7 | 8.5 | 140 | 360 | -1.85 | .170 | 12 |
| 11 | 47.0 | 21.4 | 710 | 1 800 | -2.17 | .107 | 12 |
| 12 | 4.1 | 1.9 | 970 | 2 500 | -2.26 | .158 | 12 |
| 13 | 73.4 | 33.3 | 390 | 990 | -1.88 | .102 | 12 |
| Combined | - | - | 560 | 215 | -2.04 | .234 | 129 |

[1] Log value.

During the subsequent expansion of the exploratory drift into a chamber, the Corps of Engineers used the prediction equation to help design blast rounds that would not generate excessive vibration levels.

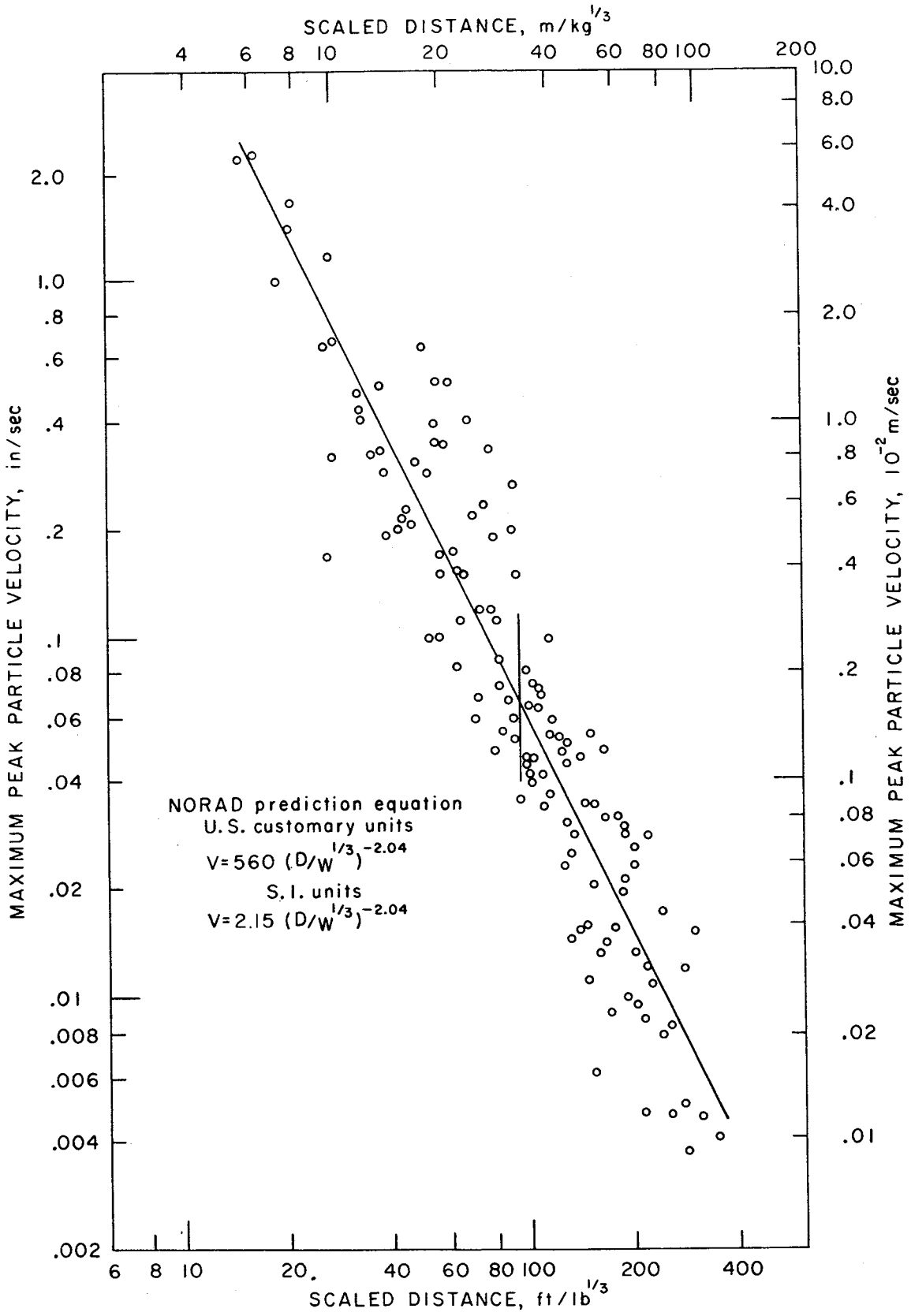


FIGURE 7. - Combined Least-Squares Regression Line–NORAD Shots 1-13.

# CONCLUSIONS

Previous Bureau studies of ground vibrations from open pit blasting (11) and of roof vibrations from underground mine blasts (15, 18) have demonstrated that the effect of the charge weight on the amplitude of the vibrations can be removed by scaling the distance by a factor (b), which was shown to be the square root of the charge weight. The analysis of variance performed on the peak particle velocity data from the blasts used to excavate the exploratory drift at NORAD showed that dividing the distance by the cube root rather than the square root of the charge weight removed the effect of the charge weight per delay on the vibration amplitudes. The 95-percent confidence interval for the scaling exponent b for the NORAD data was $0.249 \leq b \leq 0.357$.

The empirical equation, $V = 560\ (D/W^{1/3})^{-2.04}$, was obtained from the least-squares line through the combined NORAD vibration data. The equation provides an estimate of the peak particle velocities in inches per second generated by tunnel blasts in the Pikes Peak Granite of the NORAD site.

The results of the NORAD experiments, that cube-root scaling is more appropriate than square-root scaling for removing the effect of charge weight on ground vibrations, indicate that more data are needed to determine which factor should be used to design underground blasts with safe vibration levels.

## REFERENCES


1. Devine, J. F., R. H. Beck, A. V. C. Meyer, and W. I. Duvall. Effect of Charge Weight on Vibration Levels From Quarry Blasting. BuMines Rept. of Inv. 6774, 1966, 37 pp.

2. _____. Vibration Levels Transmitted Across a Presplit Fracture Plane. BuMines Rept. of Inv. 6695, 1965, 29 pp.

3. Duvall, W. I., J. F. Devine, C. F. Johnson, and A. V. C. Meyer. Vibrations From Blasting at Iowa Limestone Quarries. BuMines Rept. of Inv. 6270, 1963, 28 pp.

4. Duvall, W. I., and D. E. Fogelson. Review of Criteria for Estimating Damage to Residences From Blasting Vibrations. BuMines Rept. of Inv. 5968, 1962, 19 pp.

5. Duvall, W. I., C. F. Johnson, A. V. C. Meyer, and J. F. Devine. Vibrations From Instantaneous and Millisecond Delayed Quarry Blasts. Rept. of Inv. 6151, 1963, 34 pp.

6. Hartman, I., J. Nagy, and H. C. Howarth. Experiments on Multiple Short-Delay Blasting of Coal (in Two Parts). Part I. BuMines Rept. of Inv. 4868, 1952, 16 pp.

7. Howard, T. E. Report on Hard Rock Tunnelling. Working Documents Prepared for the Advisory Conference on Tunnelling. Organization for Economic Cooperation and Development, June 22-26, 1970, Washington, D.C., pp. 12-14. (Clearinghouse No. PB 193286.)

8. Howes, M. H. Methods and Costs of Constructing the Underground Facility of North American Air Defense Command at Cheyenne Mountain, El Paso County, Colo. BuMines Inf. Circ. 8294, 1966, 69 pp.

9. Nagy, J., I. Hartman, F. P. Cristofel, and E. C. Seiler. Experiments on Multiple Short-Delay Blasting of Coal (in Two Parts). Part II. BuMines Rept. of Inv. 4875, 1952, 22 pp.

10. Nicholls, H. R., and D. E. Fogelson. Controlling Seismic Effects of Blasting. Nat. Safety Cong. Trans., 1967, pp. 46-53.

11. Nicholls, H. R., C. F. Johnson, and W. I. Duvall. Blasting Vibrations and Their Effects on Structures. BuMines Bull. 656, 1971, 105 pp.

12. Obert, L. Latest Developments in the Bureau of Mines Research Related to Damage Criterion, Presplitting, and Short-Delay Blasting. Pit and Quarry, v. 58, No. 7, January 1966, pp. 162-165, 192.

13. Ogden, L. General Geologic Report of Colorado Springs, Site A, NORAD. Parsons, Brinkerhoff, Quade and Douglas, April 1960, 17 pp.

14. Olson, J. J., and R. A. Dick. Blast Vibration Studies at Shullsburg Mine, Wisconsin. Canadian Mining J., v. 92, No. 7, July 1971, pp. 49-53.

15. Olson, J. J., R. A. Dick, J. L. Condon, A. D. Hendrickson, and D. E. Fogelson. Mine Roof Vibrations From Underground Blasts. BuMines Rept. of Inv. 7330, 1970, 55 pp.

16. Olson, J. J., R. A. Dick, D. E. Fogelson, and L. R. Fletcher. Mine Roof Vibrations From Production Blasts, Shullsburg Mine, Shullsburg, Wis. BuMines Rept. of Inv. 7462, 1970, 35 pp.

17. Olson, J. J., and L. R. Fletcher. Airblast Overpressure Levels From Confined Underground Production Blasts. BuMines Rept. of Inv. 7574, 1971, 24 pp.

18. Olson, J. J., and D. E. Fogelson. Rock Mechanics Can Help Underground Blasting Practice. Min. Eng., v. 21, No. 9, September 1969, pp. 89-92.

19. Stehlik, C. J. Mine Roof Rock and Roof Bolt Behavior Resulting From Nearby Blasts. BuMines Rept. of Inv. 6372, 1964, 33 pp.

20. Thoenen, J. R., and S. L. Windes. Earth Vibrations Caused by Mine Blasting. BuMines Rept. of Inv. 3407, 1938, 46 pp.

21. _____. Seismic Effects of Quarry Blasting. BuMines Bull. 442, 1942, 83 pp.

22. Underwood, L. B., and C. J. Distefano. Development of a Rock Bolt System for Permanent Support at NORAD. SME Trans., March 1967, pp. 30-55.

INT.-BU.OF MINES, PGH., PA. 17636